Hindawi
Adsorption Science & Technology
Volume 2022, Article ID 5257960, 10 pages
https://doi.org/10.1155/2022/5257960

Research Article

Highly Efficient and Selective Capture of Pb(II) by New Crosslinked Melamine-Based Polymethyl Methacrylate for Water Treatment

Nazeeha S. Alkayal

King Abdulaziz University, Faculty of Science, Chemistry Department, P.O. Box 80203, Jeddah 21589, Saudi Arabia

Correspondence should be addressed to Nazeeha S. Alkayal; nalkayal@kau.edu.sa

Received 1 March 2022; Revised 20 May 2022; Accepted 29 July 2022; Published 22 August 2022

Academic Editor: Ming Hua

Owing to the recent developments in the polymer's properties and application, the demands for designing different structure of polymers are greater than ever. Crosslinked polymers (CPs) are a type of porous materials that have a variety of potential applications. Because of simple methods of modification of polymethyl methacrylate (PMMA), the crosslinked PMMA considers the most commonly polymeric adsorbents. A new crosslinked melamine-based polymethyl methacrylate (C-PMMA/Mel) was prepared via a polycondensation reaction between PMMA and melamine used as a crosslinking agent. Different characterization methods were carried out to investigate the molecular structures, thermal stability, and morphology. C-PMMA/Mel was applied for the adsorption behavior toward different metal cations and detected a selective to Pb(II). The evaluation of the new polymers as adsorbent against Pb(II) ion was studied using the contact time, adsorbent dose, initial concentration, and effects of pH. The adsorption efficiency of heavy metals was improved in the presence of melamine in polymeric matrix. The C-PMMA/Mel has high efficacy in the removal of ~94% of Pb at pH 6 for one hour. Noticeably, the adsorption performance of C-PMMA/Mel perfectly suited with Freundlich isotherm and the pseudo-second-order kinetic model. Additionally, the new materials showed no obvious loss in Pb(II) removal after 7 cycles.

1. Introduction

Today, water pollution has become a key issue of world environmental concern [1]. Heavy metal ion pollution is considered to be the most hazardous substance in wastewater while they are not biodegradable and due to food chain will be collected in living organisms (including humans), causing serious environmental pollution and many diseases. It is threatening the ecosystem that can cause and pose damage and risk to other organisms. This prompted the scientists to further develop more new technologies in the areas of environmental remediation and protection [2]. Water pollution with Pb(II) is a serious concern in the field of health and increasing environmental problems due to its extremely high toxicity even at low concentrations. The main industrial sources of lead heavy metals are the industry of tanning, electroplating, textile, and leather. Lead must be considerably separated from wastewater before it is distributed into the environment or before it needs to be reformed in a less toxic form [3, 4].

Different methods primarily used to remove Pb(II) involve ion exchange, reverse osmosis, chemical precipitation, and electrodeposition [1, 5]. In very dilute solutions, these methods are not only unsuccessful for water remediation but also to be very high cost for removal of Pb(II). Therefore, many approaches have been reported to develop more effective techniques for removing lead from wastewater, for instance, liquid extraction, membrane cleaners, and adsorption [3, 6–8].

However, the most cost-effective processes and safest and direct approaches to efficiently eliminate heavy metals from wastewater are the solid adsorbents that depend on the properties of the adsorbents used. Several materials are considered as adsorbents and are divided into natural and

synthetic adsorbents, involving inorganic and organic [9]. Nevertheless, these adsorbents have the disadvantage of low capacity and long equilibrium time. Therefore, higher capacity sewing material in less time is considered a water treatment challenge. Recently, there has been enhanced interest using polymeric materials for water treatment from heavy metals due to the ability to create an active motif on their chains to enhance the capability for better adsorption [10–12].

The important class of porous materials is crosslinked polymers (CPs) that can be applied in adsorption applications because of low density, high surface area, and large stability [13]. CPs also consist of inexpensive components and are highly stable and scalable. In addition, these materials have excellent thermal and chemical stability and can be prepared on a large amount [14–16]. Crosslinked polymethyl methacrylate is considered as one of the very important polymeric adsorbents due to simple modification methods, and the chemical modifications of PMMA can improve the physical and chemical properties with different functionalities. A few studies have been conducted using crosslinked PMMA as an absorbent material for environmental applications [17–19].

Owing to the features of melamine like nitrogen content, high surface area, tunable basic functionalities, great porosity, and relatively low-cost starting materials remain an interesting field of research in polymer chemistry [20, 21]. Melamine-based polymeric materials have attracted considerable attention used as an absorbent material to make novel potential applications [22–26]. This study designed to use the (triamine) melamine as a crosslinker for PMMA to prepare new crosslinked PMMA, termed C-PMMA/Mel using polycondensation methods. Then, the new materials were applied as adsorbents towards heavy metals for water treatment. This attempt opens the research gate toward outstanding adsorbents with good properties that can suffer the limitations stated above. Overall, this research presents a new approach for constructing low-cost adsorbents and high efficiency to remove heavy metals, and it can be applied for environmental treatment.

2. Experimental

2.1. Materials. Poly (methyl methacrylate) (PMMA, M_{wt} = 300k) has been obtained from Alfa Aesar. Dimethyl sulfoxide (DMSO 99%) and melamine (97.5%) were purchased from BDH laboratory reagents. $Zn(NO_3)_2{\cdot}6H_2O$ (99%), $Cd(NO_3)_2{\cdot}4H_2O$ (99%), $Pb(NO_3)_2{\cdot}6H_2O$ (99%), and $MnCl_2{\cdot}4H_2O$ (98%) were supplied by Fisher chemicals; $NiCl_2{\cdot}6H_2O$ (97%) was supplied by BDH chemicals; $Ba(NO_3)_2{\cdot}4H_2O$ (99%) was provided by Ward's Natural Science. $Cr(NO_3)_3{\cdot}9H_2O$ (97%) was provided by Panreac and NaOH and HCl (35%) supplied from LOBA Chemie. All chemicals were used without further purifications.

2.2. Synthesis of C-PMMA/Mel. An evacuation-argon-backfill cycle was applied three-necked flask connected with a condenser and magnetic stirrer. So, 1 g of PMMA and different amounts of melamine (10, 20, and 30%) were added into 30 mL DMSO and heated to 175°C for three days under argon flow. Then, the product was collected by filtration after cooling and washed with methanol, THF, and dichloromethane to give a yield = 85%.

Table 1: Chemical compositions of PMMA and melamine for C-PMMA/Mel(1–3).

Sample	*w*/*w*% PMMA	*w*/*w*% melamine
C-PMMA/Mel1	90	10
C-PMMA/Mel2	80	20
C-PMMA/Mel3	70	30

2.3. Adsorption Study. To study the adsorption of polymer, a standard solution (20 mg/L) of different metal nitrates/chlorides was prepared. $MnCl_2{\cdot}4H_2O$, $Pb(NO_3)_2{\cdot}6H_2O$, $NiCl_2{\cdot}6H_2O$, $Cd(NO_3)_2{\cdot}4H_2O$, $Cr(NO_3)_3{\cdot}9H_2O$, $Ba(NO_3)_2{\cdot}4H_2O$, and $Zn(NO_3)_2{\cdot}6H_2O$ were dissolved in deionized water (DI) under continuous mixing. 20 mg of C-PMMA/Mel was added into 100 mL of the standard solution and stirred for one hour followed by filtration. The concentrations of metals were measured by ICP using adsorption capacity q_e (mg/g), q_t (mg/g), and the removal efficiency R% calculated according to the following equations.

$$q_e = \frac{\left(C_i - C_f\right) V}{m}, \tag{1}$$

$$q_t = \frac{\left(C_i - C_t\right) V}{m}, \tag{2}$$

$$R\% = \frac{C_i - C_f}{C_i} \times 100, \tag{3}$$

where the amount of adsorbent represents as m (g), C_i is the initial concentrations of metal cations (mg/L), C_t is the concentrations of metal cations after time, and C_f is the final concentrations of metal cations (mg/L). V is the volume (L) of the solution. To study the effect of the adsorbent efficiency to remove the heavy metals, different factors were utilized such as effect of different metals, pH value, contact time, initial concentration of Pb^{2+}, and adsorbent dosage.

2.3.1. pH Effect. At different pH values 3, 4, 5, 6, and 7, a standard solution 20 mg/L Pb(II) was prepared. To adjust the pH of the metal solution, 1 M NaOH and 1 M HCl were used. Then, at each pH value, 20 mg of C-PMMA/Mel2 was added into 100 mL of Pb(II) solution for 1 h.

2.3.2. Effect of Adsorbent Dose. Different adsorbent dose 10, 20, 30, and 40 mg of C-PMMA/Mel2 was weighted and added to 100 mL of 20 mg/L Pb(II) solution for examining the adsorption of Pb(II) ions at pH = 6.

2.3.3. Effect of Contact Time. In 100 mL of 20 mg/L Pb(II) solution, a sequence of time 10, 30, 60, 90, and 120 min was tested to study Pb(II) removal using 20 mg adsorbent in each at pH = 6.

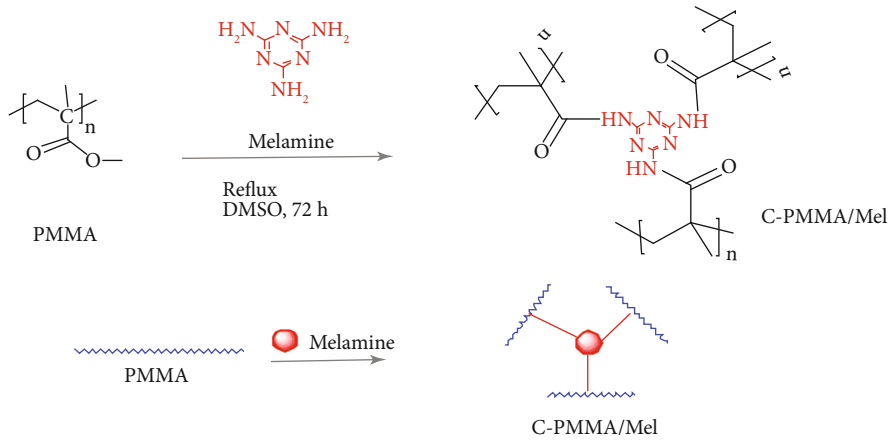

Figure 1: Synthetic routes to prepare C-PMMA/Mel.

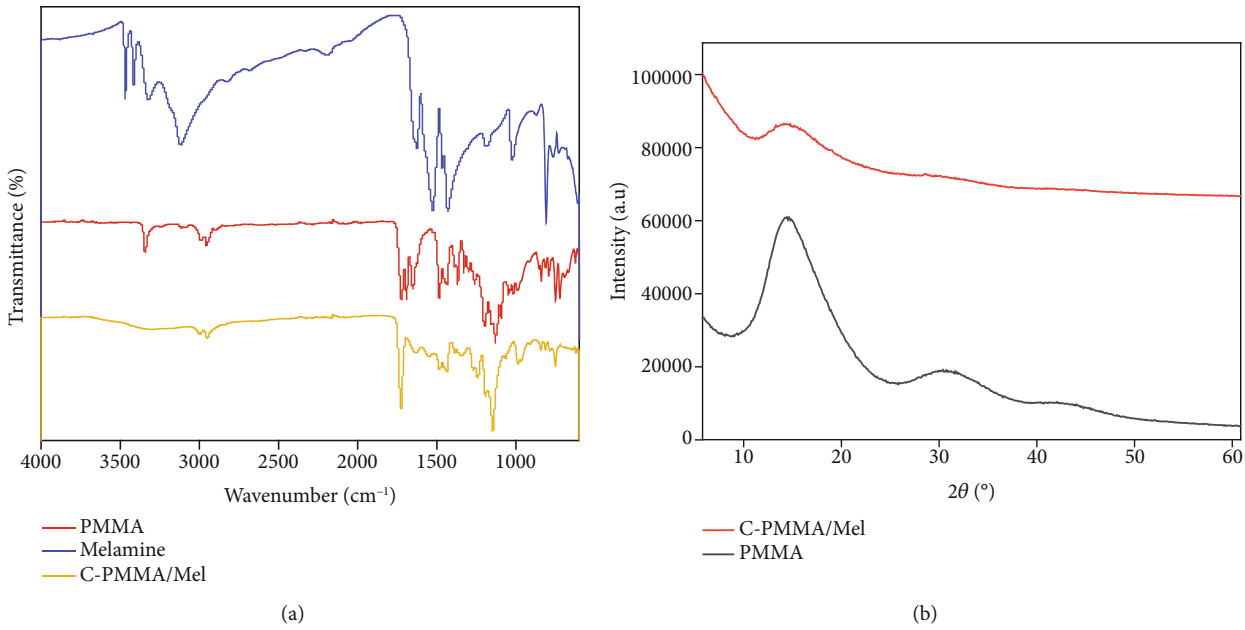

Figure 2: (a) FTIR spectra of the C-PMMA/Mel2. (b) XRD pattern of pure PMMA and the synthesized C-PMMA/Mel2.

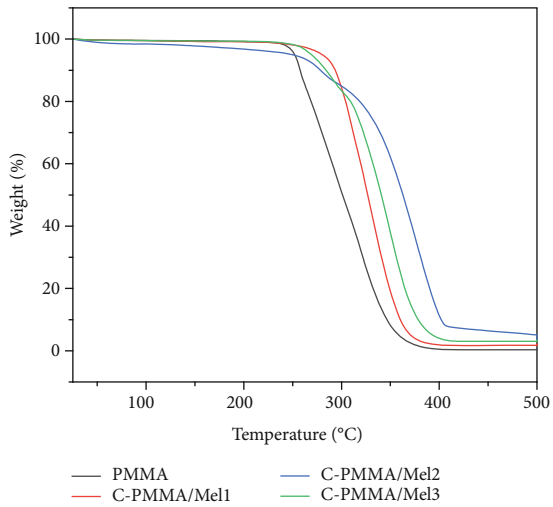

Figure 3: TGA micrograph of pure PMMA and C-PMMA/Mel(1–3).

Table 2: Thermal properties of pure PMMA and C-PMMA/Mel(1–3).

Sample	T_{10}	T_{30}	T_{50}
Pure PMMA	345	315	300
C-PMMA/Mel1	360	340	330
C-PMMA/Mel2	405	385	365
C-PMMA/Mel3	380	360	345

2.3.4. Effect of Initial Concentration. A series of concentration of Pb^{2+} solutions 5, 10, 20, 50, 100, and 200 mg/L were prepared to study Pb(II) removal in 100 mL at pH = 6 and 20 mg adsorbent for 1 h.

2.3.5. Reusability of C-PMMA/Mel2. In the desorption experiment, 50 mL HCl (0.5 M) and 50 mL ethanol were used for desorption method to renew the adsorbent from

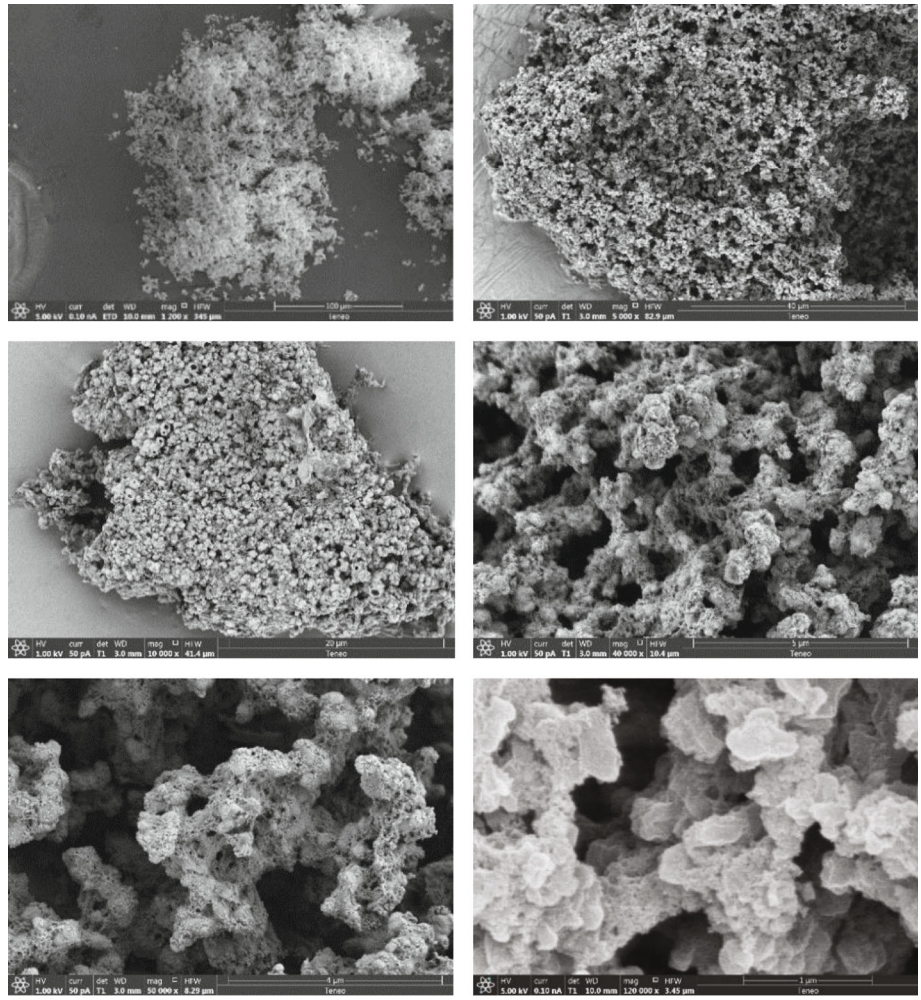

Figure 4: SEM micrographs for C-PMMA/Mel2 at different magnifications.

the Pb(II)@ C-PMMA/Mel complex. After stirring for 3 h at 25°C, the sample was rinsed using DI water then recycled using the adsorption–desorption process. The adsorption–desorption cycle was repeated 7 times.

2.4. Instrumentation. Thermogravimetric analysis (TGA) was performed on TGA4724 with a heating rate of 10°C/min between 25 and 500°C under N_2 atmosphere. Fourier transform infrared spectra (FTIR) with a Nicolet Magna 6700 FT spectrometer were conducted in a wavenumber region (400-4000 cm^{-1}). X-ray diffraction (XRD) patterns were studied using a Bruker D8 Advance with Cu Kα radiation (wavelength 1.5418 Å) at 40 kV and 40 mA. The patterns were collected between 2θ of 10° and 60°, and the scan speed was 1.5 degree/min. Scanning electron microscopy (SEM) imaging was performed with a FEI TENEO VS microscope equipped with an EDAX detector. Polymer sample was mounted on the aluminium stub using adhesive carbon tape and sputter coated with 3 nm iridium to avoid sample charging during imaging. Inductively coupled plasma optical emission spectroscopy (ICP-AES) on a PerkinElmer Optima 7000 DV was utilized to determine the metal contents.

3. Results and Discussion

3.1. Structural Investigation. As listed in Table 1, PMMA was chemically reacted with different ratios from aromatic triamines (melamine) as a crosslinking agent to create C-PMMA/Mel(1–3) by the polycondensation technique in the presence of DMSO as a solvent at 175°C for 72 h. Figure 1 illustrates the schematic representation of the crosslinking process to prepare C-PMMA/Mel.

FTIR spectroscopy investigates the connections between PMMA and the melamine as crosslinking agent for the new polymer from the range 600 to 4000 cm^{-1} as displayed in Figure 2(a). The spectrum of linear PMMA showed that the stretching vibrations (C–H) in CH_3 and CH_2 have absorption peaks at 2993 and 2948 cm^{-1}, respectively [27]. The signal of carbonyl group (C=O) stretching vibration appeared as a sharp peak around 1725 cm^{-1}. Peaks at 1242 and 1149 cm^{-1} are attributed to the stretching vibration (C-C-O) of –O–CH_3. The peaks of primary amino groups in the melamine appeared at wavelength 3442-3360 cm^{-1}. FTIR spectra of C-PMMA/Mel2 demonstrate the formation of amide bonds by the presence of

Table 3: Adsorption capacities q_e (mg/g) of C-PMMA/Mel(1–3) and removal efficiency (R%) toward different metal ions at initial pH = 6 and adsorbent dose of 20 mg.

Sample	Metal ion	q_e (mg/g)	Removal efficiency (R%)
C-PMMA/Mel1	Pb(II)	43.479	71.96
	Cr(III)	2.337	32.53
	Mn(II)	4.3485	12.79
	Ba(II)	8.1255	10.76
	Cd(II)	10.6115	21.84
	Ni(II)	3.592	16.61
	Zn(II)	6.665	20.17
C-PMMA/Mel2	Pb(II)	88.67	93.96
	Cr(III)	2.49	24.27
	Mn(II)	6.78	19.97
	Ba(II)	17.68	23.42
	Cd(II)	11.75	24.19
	Ni(II)	4.68	21.64
	Zn(II)	7.04	21.30
C-PMMA/Mel3	Pb(II)	38.1725	63.17
	Cr(III)	2.402	23.41
	Mn(II)	5.0525	14.86
	Ba(II)	10.916	14.46
	Cd(II)	9.4	19.35
	Ni(II)	3.926	18.16
	Zn(II)	6.2945	19.05

bands at 3365 and 1188 cm^{-1} assigned to the stretching vibrations and deformation vibrations of secondary amine (NH) [17, 19].

Figure 2(b) reveals the XRD patterns of the pure PMMA and the synthesized C-PMMA/Mel2. The diffractograms of XRD were analyzed in the 2θ range from 10° to 60°. The broadened peaks at 43°, 30°, and 15° are assigned for pure PMMA. The peak of C-PMMA/Mel2 crosslinked polymer was found to be a broad peak and absence of any sharp peaks observed related to melamine. According to the high level of crosslinking interaction between PMMA and melamine, the XRD diffractogram of new polymer differs from pure melamine [28] and the loss of the melamine sharp peaks.

3.2. Thermal Study. As demonstrated in Figure 3, the thermal stability of pure PMMA and C-PMMA/Mel(1–3) crosslinked polymers was investigated by TGA. The TGA curve of pure PMMA reveals that the degradation occurs mainly in one step ranged between 250°C and 345°C. The result shows a considerable increase in the thermal presentation of polymer network C-PMMA/Mel(1–3) compared to the pure PMMA, and the crosslinking influenced on the stability of polymer. T_{50}, T_{30}, and T_{10} are the temperature of percentages of decomposition that explain the mass loss of 50%, 30%, and 10%, respectively, as listed in Table 2. T_{50}, T_{30}, and T_{10} of C-PMMA/Mel(1–3) were higher than those of pure PMMA. It is observed that C-PMMA/Mel2 has the highest thermal stability than C-PMMA/Mel1 and C-PMMA/Mel3.

3.3. Morphological Investigation. Scanning electron microscope (SEM) measurements were typically applied to assess the surface of C-PMMA/Mel as shown in Figure 4. Pure PMMA was displayed as a smooth surface [29] while the pure melamine shows an irregular stone-like structure with a size of ten micrometers [28]. As an example, the SEM image of C-PMMA/Mel2 crosslinked polymer shows in micrometer range a roughness surface with pores with irregular tiny particles. With the addition of melamine as a crosslinker, the surface morphology of PMMA significantly changed from smooth to amorphous character with increased porosity and deformation of the circular holes confirming the excellent interaction between melamine and PMMA and the crosslinking process effectively occurred.

3.4. Metal Adsorption. Table 3 shows the adsorption capacities (mg/g) of C-PMMA/Mel(1–3) toward different metal cations and C-PMMA/Mel(1–3) has very good uptake with superior selectivity towards Pb(II) cation as displayed in Figure 5. The significant Pb(II) adsorption capacity observed by C-PMMA/Mel(1–3) is a major phenomenon may be due to the following: (i) amino groups can very effectively bind to the Pb(II) cation, since they act as coordinating ligands [26]; (ii) the specific surface shape and random structures are very useful for the adsorption of heavy metal ions [30]. According to the highest adsorption capacity of C-PMMA/Mel2 toward Pb(II), C-PMMA/Mel2 and Pb(II) cation were selected for the following adsorption experiments.

The effect of pH on Pb^{2+} removal is shown in Figure 6(a). The adsorption capacity increases while pH increases from pH 3 to 6 and then decreases at pH = 7. As a result, the addition of an acid that protonates the nitrogen atom of C-PMMA/Mel2 creates a positively charged surface that electrostatically repels metal ions [31]. If the pH is increased, the surface charge of the polymer converted into negative due to the nitrogen atom is totally deprotonated. Therefore, the adsorption capacities of Pb(II) were considerably elevated due to the electrostatic attractions between ions of different charges [32]. However, when pH exceeds 6, OH- interacts with Pb(II) cations, resulting in the production of $PbOH^+$ and $Pb(OH)_2$. Under these conditions, the mechanism of Pb(II) removal becomes more difficult, and it becomes difficult to distinguish the precipitation and adsorption of Pb(II) in solution [33]. Thus, at pH 6 the maximum adsorption capability for Pb^{2+} removal was found 88.67 mg/g by C-PMMA/Mel2 crosslinked polymer which was then used in the following adsorption studies.

Different adsorbent dosages from10 to 40 mg were applied as shown in Figure 6(b). The maximum adsorption capacity was 84.5 mg/g using adsorbent dose 20 mg used in further adsorption experiments. The influence of different initial concentrations of Pb(II) on adsorption

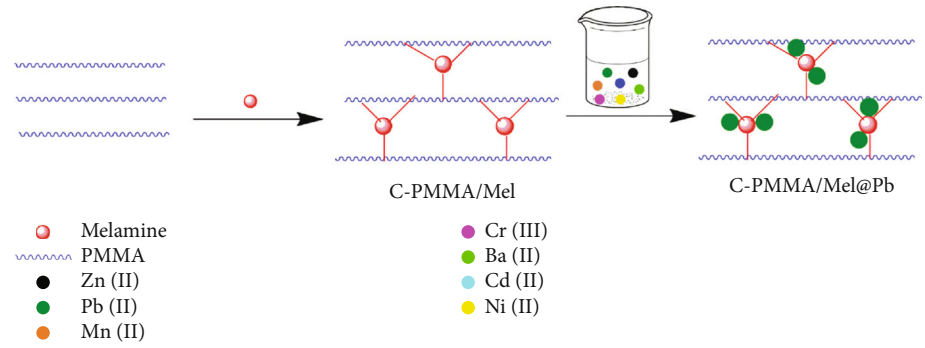

Figure 5: Schematic illustrations of the newly synthesized C-PMMA/Mel on the removal of Pb(II).

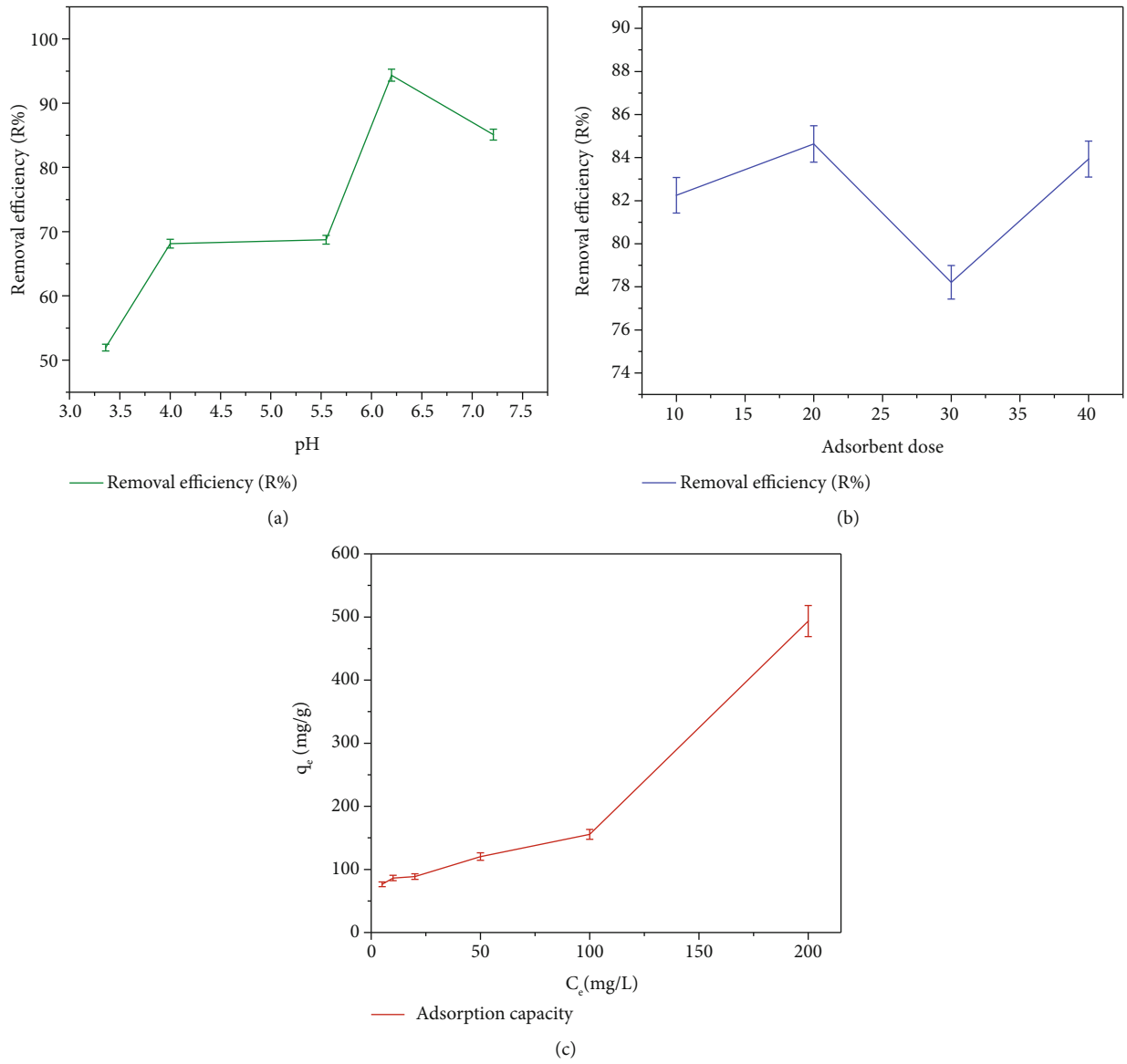

Figure 6: Impact of (a) pH, (b) initial concentration of Pb^{2+} metal ions, and (c) C-PMMA/Mel2 dose of Pb(II) adsorption.

capability of C-PMMA/Mel2 for Pb^{2+} is revealed in Figure 6(c) (20 mg of adsorbent, pH 6.0). Clearly, q_e increased from 80 to 450 mg/g while the concentration raised from 0 to 200 mg/L. In order to study Pb(II) removal at low concentration, 20 mg/L was used in further adsorption experiments.

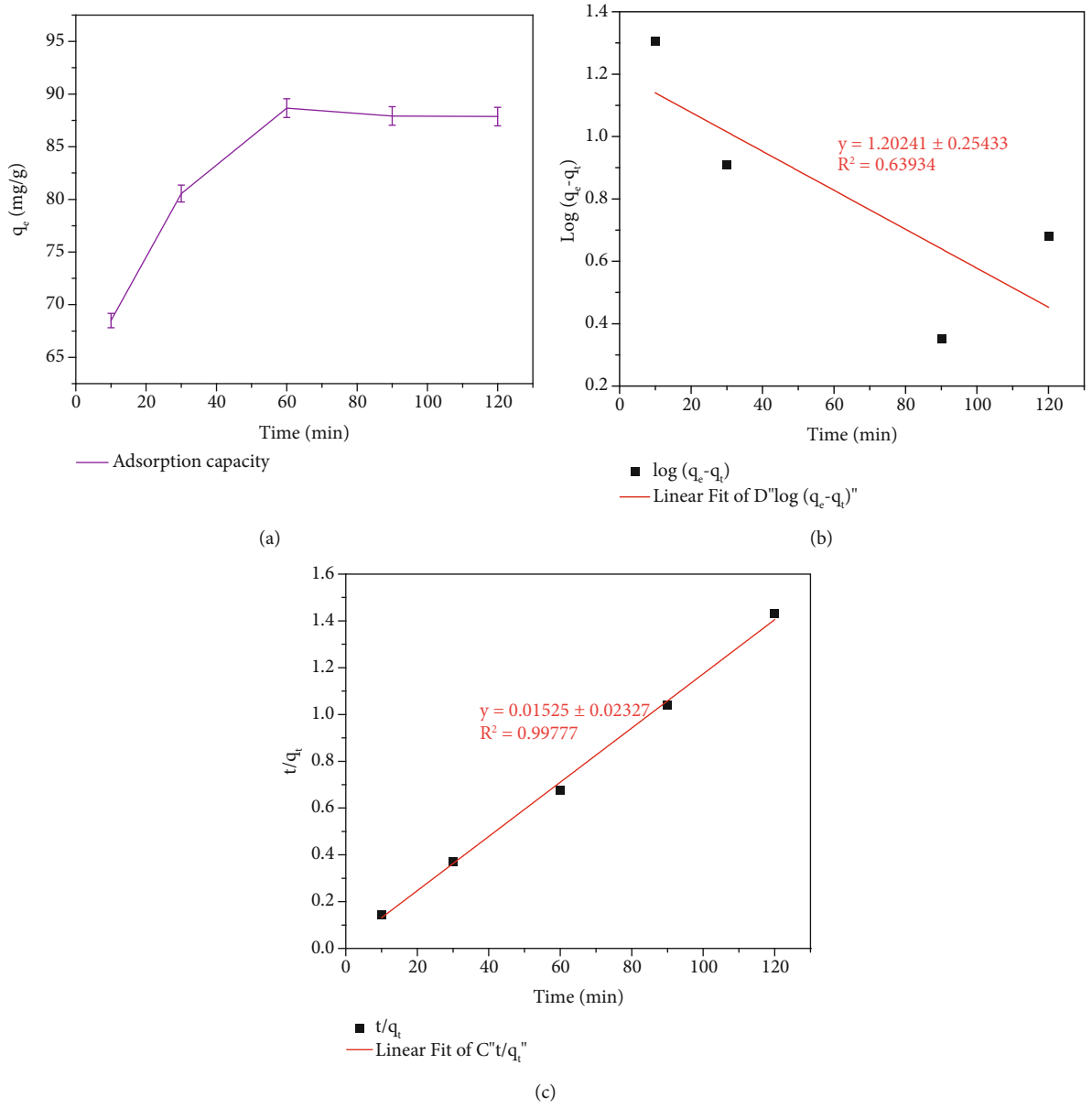

Figure 7: (a) Impact of contact time on removal of Pb(II). (b) Pseudo-first-order. (c) Pseudo-second-order.

3.5. Adsorption Kinetics. To study the adsorption ability of a polymer adsorbent, the kinetic method was carried out by immersing 20 mg of C-PMMA/Mel2 into 100 mL of a Pb^{2+} solution (20 mg/L, pH 6.0) at 25°C.

As found in Figure 7(a), the adsorption of Pb(II) rapidly happened in the first 60 minutes, and the equilibrium was reached after 120 minutes. The adsorption behavior of C-PMMA/Mel2 is most likely due to its porous network architecture, and the pseudo-first-order model (PFO) and the pseudo-second-order model (PSO) were carried out to analyze the adsorption dynamic in Figures 7(b) and 7(c).

Pseudo-first-order model:

$$\log(q_e - q_t) = \log(q_e) - \frac{K_1 t}{2.303}. \quad (4)$$

Pseudo-second-order model:

$$\frac{t}{q_t} = \frac{t}{q_e} + \frac{1}{K_2 q_e^2}, \quad (5)$$

where q_e, q_t (mg/g) are the adsorption capacity at equilibrium and the adsorption capacity at time (min), respectively. k_1 (min^{-1}) and k_2 (g/mg·min) are the rate constants in PFO and PSO models, respectively. Consistent with the PFO and PSO models, the linear plots of $\ln(q_e - q_t)$ or (t/q_t) against time (min) are illustrated in Figures 7(b) and 7(c). By comparing the correlation coefficient (R^2) for PFO and PSO, the value of the PFO model (0.63934) was lower than that of the PSO model (0.99777), demonstrating that the adsorption process of Pb(II) was controlled by chemisorption mechanism [34].

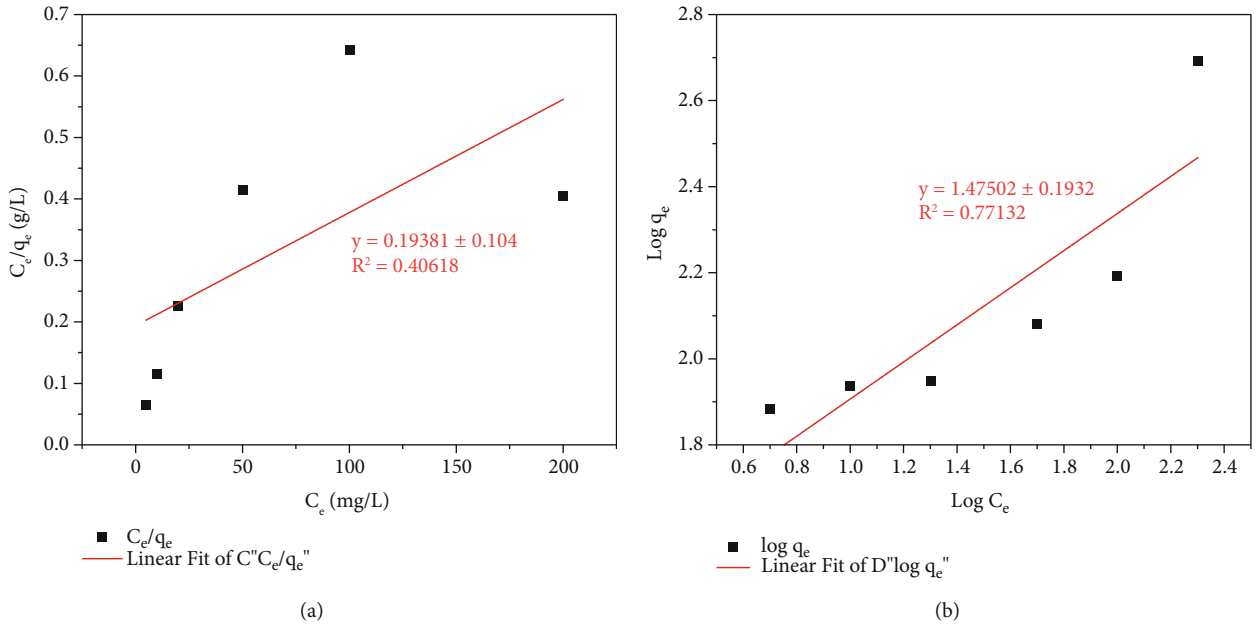

Figure 8: (a) Langmuir model and (b) Freundlich model for Pb^{2+} adsorption.

Table 4: Comparison between various adsorbents on the adsorption capacities q_e (mg/g) for Pb(II) removal.

Adsorbent	q_e (mg/g)	Ref.
PMMA-*g*-Alg/Fe_3O_4	62.50	[37]
PEI-immobilized PMMA microspheres	28.32	[38]
Melamine-vanillin polymer (MVP)	8.53	[25]
Melamine- pyridine polyaminal network (MA-Py)	53.13	[26]
C-PMMA/Mel2	88.67	This study

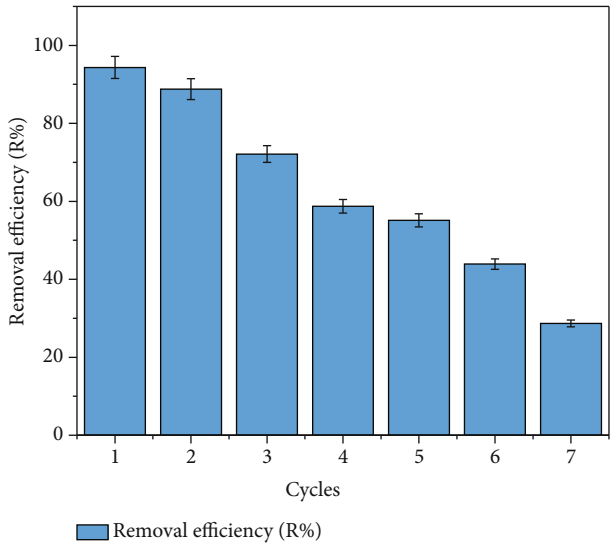

Figure 9: Adsorption–desorption recycles of Pb(II) (m = 20 mg, V = 100 mL, pH = 6, and initial concentration of Pb(II) = 20 mg/L).

3.6. Adsorption Isotherms. To estimate the interaction properties between adsorbent and adsorbate, isotherm models have been extensively utilized [35]. The equations of Langmuir and Freundlich models are presented as follows:

$$\frac{C_e}{q_e} = \frac{C_e}{q_m} + \frac{1}{bq_m}, \tag{6}$$

$$\log q_e = \log k_F + \frac{1}{n} \log C_e, \tag{7}$$

where q_e (mg/g) symbolizes the equilibrium sorption capacity, q_m (mg/g) reveals the maximum adsorption capacity, b and K_F (L/mg) are the Langmuir and Freundlich constants, respectively, and the equilibrium concentration in solution is C_e (mg/L). Figures 8(a) and 8(b) demonstrate the Langmuir and Freundlich schemes for C-PMMA/Mel2 on Pb(II) adsorption. Noticeably, the R^2 value (0.77132) for Freundlich model is higher than the R^2 value (0.40618) of Langmuir model. Therefore, the adsorption methods of C-PMMA/Mel2 for Pb(II) were clearer defined by the Freundlich model, representing the multilayer adsorption of Pb(II) onto C-PMMA/Mel2 [36].

Various adsorbents with the new adsorbent in this study are listed in Table 4 for comparing the adsorption capacities towards Pb(II). Thus, the current adsorbent has great adsorption capacities, and it can be effectively used for removal of Pb(II) from wastewater.

To study the effectivity of the treatment method, adsorbent recycling was applied. As shown in Figure 9, the polymer can be recycled a maximum of three times without

losing its efficiency after performing the adsorption and desorption method seven times. The removal efficiency after three recycling runs at optimum conditions was 94%, 88%, and 74%, respectively.

4. Conclusions

A new crosslinked melamine-based PMMA has been synthesized, and the results demonstrated a selective absorbent property against Pb(II) from aqueous solutions. Different techniques such as XRD, FTIR, TGA, and SEM were utilized to characterize the new material. The structural study confirmed the chemical interaction between PMMA and melamine, while the morphological analysis proved the formation of crosslinked C-PMMA/Mel, followed by the evaluation of the new crosslinked as adsorbent for Pb(II) using different pH value and the adsorbent dose. As a result, the new crosslinked polymer has high adsorbing efficiency for Pb(II) removal at one hour with removal efficiency equaled 94% at pH value equaled 6. This attempt opens the door toward outstanding adsorbents with good properties and low cost for removing heavy metals, and it can be applied for environmental treatment.

Data Availability

No data were used to support this study.

Conflicts of Interest

The author declares that there are no conflicts of interest.

Acknowledgments

This research work was funded by Institutional Fund Projects under grant no. IFPDP-244-22. Therefore, the author gratefully acknowledges the technical and financial support from the Ministry of Education and Deanship of Scientific Research (DSR), King Abdulaziz University (KAU), Jeddah, Saudi Arabia.

References

[1] M. I. Inyang, B. Gao, Y. Yao et al., "A review of biochar as a low-cost adsorbent for aqueous heavy metal removal," *Critical Reviews in Environmental Science and Technology*, vol. 46, no. 4, pp. 406–433, 2016.

[2] L. Joseph, B. M. Jun, J. R. Flora, C. M. Park, and Y. Yoon, "Removal of heavy metals from water sources in the developing world using low- cost materials: a review," *Chemosphere*, vol. 229, pp. 142–159, 2019.

[3] M. R. Karim, M. O. Aijaz, N. H. Alharth, H. F. Alharbi, F. S. Al-Mubaddel, and M. R. Awual, "Composite nanofibers membranes of poly(vinyl alcohol)/chitosan for selective lead(II) and cadmium(II) ions removal from wastewater," *Ecotoxicology and Environmental Safety*, vol. 169, pp. 479–486, 2019.

[4] C. Abasi, W. Donbebe, and E. D. Dikio, "Adsorption study of lead (II) ions on poly (methyl methacrylate) waste material," *Asian Journal of Chemistry*, vol. 30, no. 4, pp. 859–867, 2018.

[5] G. Z. Kyzas and M. Kostoglou, "Green adsorbents for wastewaters: a critical review," *Materials*, vol. 7, no. 1, pp. 333–364, 2014.

[6] Z. Li, T. Li, L. An, P. Fu, C. Gao, and Z. Zhang, "Highly efficient chromium(VI) adsorption with nanofibrous filter paper prepared through electrospinning chitosan/polymethylmethacrylate composite," *Carbohydrate Polymers*, vol. 137, pp. 119–126, 2016.

[7] K. Y. Kumar, T. V. Raj, S. Archana, S. B. B. Prasad, S. Olivera, and H. B. Muralidhara, "SnO_2 nanoparticles as effective adsorbents for the removal of cadmium and lead from aqueous solution: adsorption mechanism and kinetic studies," *Journal of Water Process Engineering*, vol. 13, pp. 44–52, 2016.

[8] A. Salisu, M. M. Sanagi, A. Abu Naim, W. A. Wan Ibrahim, and K. J. Abd Karim, "Removal of lead ions from aqueous solutions using sodium alginate-graft-poly(methyl methacrylate) beads," *Desalination and Water Treatment*, vol. 57, no. 33, pp. 15353–15361, 2016.

[9] P. A. Kobielska, A. J. Howarth, O. K. Farha, and S. Nayak, "Metal-organic frameworks for heavy metal removal from water," *Coordination Chemistry Reviews*, vol. 358, pp. 92–107, 2018.

[10] K. Dutta and S. De, "Aromatic conjugated polymers for removal of heavy metal ions from wastewater: a short review," *Environmental Science: Water Research & Technology*, vol. 3, no. 5, pp. 793–805, 2017.

[11] G. Zhao, X. Huang, Z. Tang, Q. Huang, F. Niu, and X. Wang, "Polymer-based nanocomposites for heavy metal ions removal from aqueous solution a review," *Polymer Chemistry*, vol. 9, no. 26, pp. 3562–3582, 2018.

[12] Y. O. Al-Ghamdi, K. A. Alamry, M. A. Hussein, H. M. Marwani, and A. M. Asiri, "Sulfone-modified chitosan as selective adsorbent for the extraction of toxic Hg (II) metal ions," *Adsorption Science & Technology*, vol. 37, no. 1-2, pp. 139–159, 2019.

[13] W. Q. Wang, J. Wang, J. G. Chen et al., "Synthesis of novel hyper-cross-linked polymers as adsorbent for removing organic pollutants from humid streams," *Chemical Engineering Journal*, vol. 281, pp. 34–41, 2015.

[14] I. A. Udoetok, R. M. Dimmick, L. D. Wilson, and J. V. Headley, "Adsorption properties of cross-linked cellulose-epichlorohydrin polymers in aqueous solution," *Carbohydrate Polymers*, vol. 136, pp. 329–340, 2016.

[15] L. Wang, Y. Zhang, H. Jiang, and H. Wang, "Carbonyl-incorporated aromatic hyper-cross-linked polymers with microporous structure and their functional materials for CO_2adsorption," *Industrial & Engineering Chemistry Research*, vol. 59, no. 36, pp. 15955–15966, 2020.

[16] L. Xie, Z. Zheng, Q. Lin et al., "Calix[4]pyrrole-based cross-linked polymer networks for highly effective iodine adsorption from water," *Angewandte Chemie International Edition*, vol. 61, no. 1, article e202113724, 2022.

[17] M. A. Hussein, H. K. Albeladi, A. S. Elsherbiny, R. M. el-Shishtawy, and A. N. al-romaizan, "Cross-linked poly(methyl methacrylate)/multiwall carbon nanotube nanocomposites for environmental treatment," *Advances in Polymer Technology*, vol. 37, no. 8, 3251 pages, 2018.

[18] A. Jakóbik-Kolon, A. Milewski, D. Zdybał et al., "Zinc sorption on modified waste poly (methyl methacrylate)," *Materials*, vol. 10, no. 7, p. 755, 2017.

[19] M. A. Hussein, M. M. Alam, H. K. Albeladi, R. M. El-Shishtawy, A. M. Asiri, and M. M. Rahman, "Nanocomposite

containing cross-linked Poly(Methyl-Methacrylate)/Multiwall carbon nanotube as a selective Y3+sensor probe," *Polymer Composites*, vol. 40, no. S2, pp. E1673–E1684, 2019.

[20] R. J. Krupadam and S. S. Rayalu, "Melamine-based resins and their carbons for CO_2 capture: a review," *Emergent Materials*, vol. 4, no. 2, pp. 545–563, 2021.

[21] D. S. Ahmed, G. A. El-Hiti, E. Yousif, A. A. Ali, and A. S. Hameed, "Design and synthesis of porous polymeric materials and their applications in gas capture and storage: a review," *Journal of Polymer Research*, vol. 25, no. 3, 2018.

[22] O. Al Hamouz, I. Adelabu, and T. Saleh, "Novel cross-linked melamine based polyamine/CNT composites for lead ions removal," *Journal of Environmental Management*, vol. 192, pp. 163–170, 2017.

[23] P. Bhanja, S. K. Das, K. Bhunia et al., "A new porous polymer for highly efficient capacitive energy storage," *ACS Sustainable Chemistry & Engineering*, vol. 6, no. 1, pp. 202–209, 2018.

[24] Y. Sang, Y. Cao, L. Wang et al., "N-rich porous organic polymers based on Schiff base reaction for CO_2 capture and mercury(II) adsorption," *Journal of Colloid and Interface Science*, vol. 587, pp. 121–130, 2021.

[25] H. G. Seong, J. Ryu, Y. Qian, J. I. So, S. H. Baeck, and S. E. Shim, "Novel hierarchically porous melamine-vanillin polymer: synthesis and application for the Pb(II) ion removal in wastewater," *Macromolecular Research*, vol. 27, no. 9, pp. 882–887, 2019.

[26] R. Sandín, M. González-Lucas, P. A. Sobarzo, C. A. Terraza, and E. M. Maya, "Microwave-assisted melamine-based polyaminals and their application for metal cations adsorption," *European Polymer Journal*, vol. 155, pp. 110562–110569, 2021.

[27] M. R. Reddy, A. R. Subrahmanyam, M. M. Reddy, J. S. Kumar, V. Kamalaker, and M. J. Reddy, "X-RD, SEM, FT-IR, DSC studies of polymer blend films of PMMA and PEO," *Materials Today*, vol. 3, pp. 3713–3718, 2016.

[28] C. Liu, X. Dong, Y. Hao, X. Wang, H. Ma, and X. Zhang, "A novel supramolecular preorganization route for improving g-C_3N_4/g-C_3N_4metal-free homojunction photocatalysis," *New Journal of Chemistry*, vol. 41, no. 20, pp. 11872–11880, 2017.

[29] M. D. Alamgir, A. Mallick, G. C. Nayak, and S. K. Tiwari, "Development of PMMA/TiO_2 nanocomposites as excellent dental materials," *Journal of Mechanical Science and Technology*, vol. 33, no. 10, pp. 4755–4760, 2019.

[30] G. Yang, H. Han, C. Du, Z. Luo, and Y. Wang, "Facile synthesis of melamine-based porous polymer networks and their application for removal of aqueous mercury ions," *Polymer*, vol. 51, no. 26, pp. 6193–6202, 2010.

[31] L. Sun, H. Yu, and B. Fugetsu, "Graphene oxide adsorption enhanced by in situ reduction with sodium hydrosulfite to remove acridine orange from aqueous solution," *Journal of Hazardous Materials*, vol. 203-204, pp. 101–110, 2012.

[32] P. K. Gautam, S. Shivalkar, and S. Banerjee, "Synthesis of M. oleifera leaf extract capped magnetic nanoparticles for effective lead [Pb (II)] removal from solution: kinetics, isotherm and reusability study," *Journal of Molecular Liquids*, vol. 305, p. 112811, 2020.

[33] Y. Liang, M. Jun, and W. Liu, "Enhanced removal of lead (II) and cadmium(II) from water in alum coagulation by ferrate (VI) pretreatment," *Water Environment Research*, vol. 79, no. 12, pp. 2420–2426, 2007.

[34] D. P. Facchi, A. L. Cazetta, E. A. Canesin et al., "New magnetic chitosan/alginate/Fe_3O_4@SiO_2 hydrogel composites applied for removal of Pb(II) ions from aqueous systems," *Chemical Engineering Journal*, vol. 337, pp. 595–608, 2018.

[35] Q. Liu, Q. Liu, B. Liu, T. Hu, W. Liu, and J. Yao, "Green synthesis of tannin-hexamethylendiamine based adsorbents for efficient removal of Cr(VI)," *Journal of Hazard Material*, vol. 352, pp. 27–35, 2018.

[36] C. B. Godiya, X. Cheng, D. Li, Z. Chen, and X. Lu, "Carboxymethyl cellulose/polyacrylamide composite hydrogel for cascaded treatment/reuse of heavy metal ions in wastewater," *Journal of Hazard Material*, vol. 364, pp. 28–38, 2019.

[37] P. E. Duru, S. Bektas, O. Genc, S. Patir, and A. Denizli, "Adsorption of heavy-metal ions on poly(ethylene imine)-immobilized poly(methyl methacrylate) microspheres," *Journal of Applied Polymer Science*, vol. 81, no. 1, pp. 197–205, 2001.

[38] A. Mittal, R. Ahmad, and I. Hasan, "Poly (methyl methacrylate)-grafted alginate/Fe_3O_4nanocomposite: synthesis and its application for the removal of heavy metal ions," *Desalination and Water Treatment*, vol. 57, no. 42, pp. 19820–19833, 2016.